

# Validation of URANS Simulations of a Small-Scale Vertical Axis Wind Turbine using OpenFOAM

Faris Al-Jamal<sup>1</sup>, Ulf Winkelmann<sup>1</sup>, Cornelia Kalender<sup>1</sup>, Rüdiger Höffer<sup>1</sup>

<sup>1</sup>*Ruhr Universität Bochum, Bochum, Germany, faris.al-jamal@rub.de*

<sup>1</sup>*ulf.winkelmann@rub.de*

<sup>1</sup>*Cornelia.Kalender@rub.de*

<sup>1</sup>*Ruediger.Hoeffler@rub.de*

## SUMMARY:

In this study, simulation results of a CFD investigation of a Vertical Axes Wind Turbine (VAWT) using the open-source code OpenFOAM (OF) are shown. 2D URANS simulations of a 3-bladed VAWT operating under various tip speed ratios were performed with the K-Omega-SST turbulence model. The main goals are to investigate the potential and limitations of OF for this application. Conclusions show that simulations using a moving mesh with an Arbitrary Mesh Interface (AMI) can be challenging, and it highly affects the meshing techniques and the solution's resolution. Despite the medium-sized mesh, the model is able to predict the experimental power coefficients and is validated against wind tunnel data.

*Keywords: CFD, OpenFOAM, VAWT*

## 1. THE BACKGROUND AND THE MOTIVATION

The increasing demand and consumption of electricity, the consequences of political instabilities on energy prices, and the stricter environmental legislation to break climate changes are the main drivers to look for alternative energy resources. Over decades the Horizontal Axes Wind Turbine (HAWT), proved their great potential as electricity generators via wind energy. Nevertheless, they cannot stand alone against the mentioned factors, as a result, the growing concept, the Vertical Axes Wind Turbine (VAWT), introduces itself as a supporting solution within urban areas. In contrast to HAWT, the rotating shaft of the VAWT is perpendicular to the wind direction, and they exist under two main categories: The drag type (Savonius), and the lift type (Darrieus) which is more complex but more efficient.

For urban applications, VAWT show enormous advantages over the HAWT such as easier maintenance, independency from the wind direction, less noise generation, and their small scale that overcomes the geographical size limitations (Rezaeiha et al., 2019). On the other hand, factors, such as standing alternating loads and vibrations, be more efficient, overcoming dynamic stall, and have a self-starting mechanism, increase their material and geometrical complexity. The great potential of the VAWT encourages further research and development. For example, adjusting the rotor diameter to increase the downwind blade's efficiency, improving the blade's aerodynamic

design, e.g., a helical shape, to produce a nearly constant torque, creating a variable blade's AOA to ensure optimal operation.

## 2. NUMERICAL METHODOLOGY | CFD SETUP

### 2.1. Geometry

The current study runs 2D-URANS airflow simulations over a 3-bladed H-Type VAWT. The turbine's components: blades (NACA0021 airfoil with chord 85mm), a shaft (diameter 40mm), and AMI (diameter 1545mm) have been designed using AutoCAD, which results in a VAWT of radius 515mm and a solidity ratio 0.247. A special geometrical care took place to ensure smoothness and avoid artificial roughness, such as taking 1000 points (instead of 200) that define each airfoil and enabling the maximum FACETRES feature in AutoCAD.

### 2.2. Spatial discretization | Meshing

The non-uniform structured background mesh has been generated using BlockMesh utility for the numerical domain. It is based on the guidelines in (Rezaeiha et al., 2019), which corresponds to 35d in x-direction, 20d in y-direction, and 0.1m in z-direction, where the VAWT's shaft has been placed in the origin with 10d distance each from the inlet, top, and bottom patches as seen in Fig. 1 on the right-hand side.

SnappyHexMesh (SHM) utility has been used to define the geometry and refine specified regions, such as the C-grid region for the airfoil, and the circular one for the AMI and the shaft. Furthermore, four layers were added with  $\max y^+ \sim 0.125$ . The final mesh shown on the left-hand side in Fig. 1 corresponds to 83k cells, however, only two meshes were used for the mesh sensitivity due to a Floating Point Error in OF for finer Meshes over 100k cells. Afterwards it was found that such problem was related to a small number of non-conforming cells (up to 10) at the AMI surface for a short period at the beginning of the simulation, namely between 0.025-0.030 seconds. Finally, the dynamicMesh utility was responsible in defining the mesh's rotational motion based on the Tip Speed Ratio  $\lambda$  ( $= 1.68 - 3.08$ ).

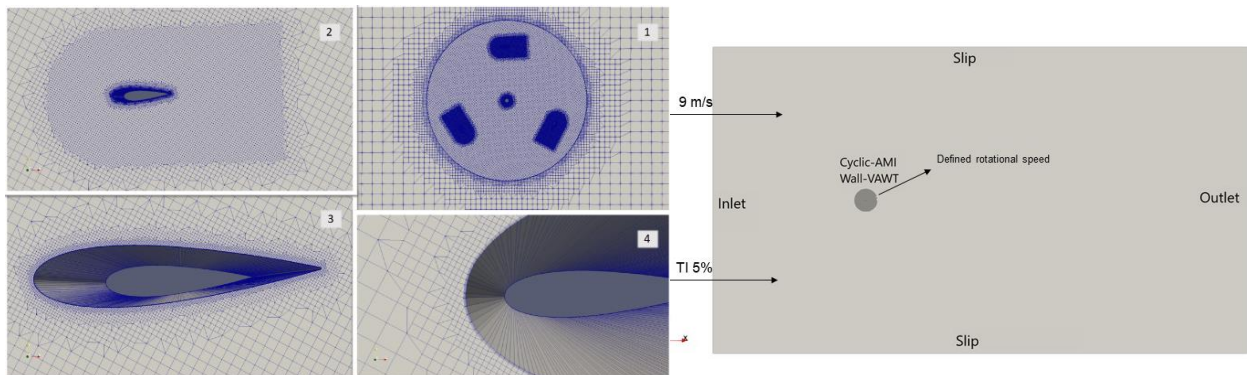


**Figure 1.** Various visualizations of the mesh around the geometries (left). Used boundary conditions (right).

### 2.3. Numerical settings | Pre-processing

Further settings include defining the boundary conditions as shown in Fig. 1 right, as well as choosing reasonable discretization schemes and solving techniques. 2<sup>nd</sup> order schemes have been

used for the temporal discretization, bounded 2<sup>nd</sup> order for the gradients, while a combination of 1<sup>st</sup> and 2<sup>nd</sup> order ones were used for the diffusion and the advection parts. The PIMPLE algorithm and the k-omega-SST model has been used to solve the system of equations. Conservative residuals of 10<sup>-7</sup> have been used for all parameters. For stability and convergence reasons a steady-RANS simulation initialized the transient one which run for time corresponds to 21 revolutions to reach a steady convergence. The time step has been changed with respect to  $\lambda$  (3.24e-5 - 5.9e-5 sec) and chosen based on (Rezaeiha et al., 2019) guidelines. It corresponds to 0.1 degrees of rotational motion per time step and 20 iterations per time step has been specified.

### 3. RESULTS AND VALIDATIONS

The simulation's convergence and the residual's drop to the specified values are monitored and checked. The simulation successfully captured the Kármán vortex street around the shaft and the physical correct aerodynamics around the turbine's blades (airfoils), such as high pressure and suction regions as well as the adverse pressure gradient, with respect to different Azimuth angle.

The behaviour of the average power coefficient ( $C_{p,avg}$ ) over the tip speed ratio ( $\lambda$ ) against the wind tunnel data (Castelli et al., 2011) is shown in Fig. 2. The validation of the power coefficient can be considered successful with an expected degree of error. The power coefficient has been calculated based on the following equation:

$$C_{p,avg} = \frac{C_{m,avg} R_{Rotor} \omega}{V_{\infty}} \quad (1)$$

Where,  $C_{m,avg}$  is the turbine's average moment coefficient including the shaft over the last revolution, which is calculated by a built-in function in OF, while  $V_{\infty}$  and  $\omega$  are the free-stream and rotational velocities, respectively.

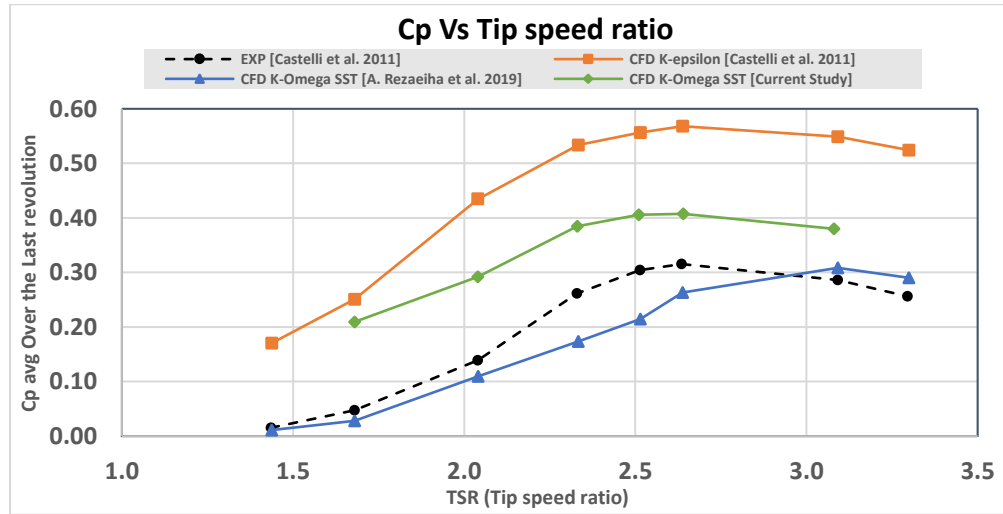


**Figure 2.** The average power coefficient versus the tip speed ratio, a comparison against the wind tunnel data as well as the CFD results from literature.

A closer look at Fig. 2 and Fig. 3 reveals helpful information for validation. First, the drop in the power coefficient in the dynamic stall region at  $\lambda = 3.08$  can be explained by the increase in the actual angle of attack (AOA) when  $\lambda$  increases. Second, one can notice in Fig. 3 the three locals

maximum of  $C_p$  within a full revolution, that corresponds to the contribution from each blade being in the upwind side and perpendicular to the wind direction. Most of the turbine's power seems to be generated within the upwind side compared to the downside, which can be spotted at time 2.9s and 2.925s, where  $C_p$  reaches a local maximum and minimum, respectively. These phenomena can be explained due to the wind's kinetic energy drops after hitting the first blade in the upwind region and the rotating shaft in the middle.

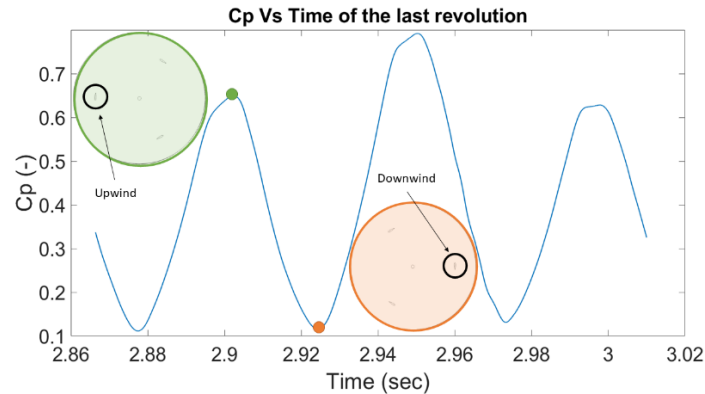


**Figure 3.** The pressure coefficient  $C_p$  over the last revolution of case  $\lambda = 2.51$ . It includes an illustration of the differences between blades' position and their effect on the  $C_p$  values.

#### 4. CONCLUSIONS AND FUTURE WORK

The current study validates the URANS simulations of a 3-bladed VAWT operating under various tip speed  $\lambda$  using OpenFOAM with the K-Omega-SST turbulence model. The main goals were to investigate different features of meshing and solving on OpenFOAM, and to ensure the reliability of that model. When using a rotating mesh the simulation might crash under the Floating Point Error, however, careful definition of the Arbitrary Mesh Interface (AMI) can eliminate such issue. After reaching the desired convergence, the results were successfully validated against literature data (Castelli et al., 2011) (Rezaeiha et al., 2019), despite the incomplete mesh sensitivity. Finally, the turbine's power performance and some aerodynamic analyses were made.

As following work, the effect of the shaft on the aerodynamic performance of the VAWT will be analysed and possible improvements through manipulating the shaft's roughness will be explored.

#### REFERENCES

- Greenshields, C and Weller, H., 2022. Notes on Computational Fluid Dynamics: General Principles. CFD Direct Ltd, Reading, UK.
- Raciti Castelli, M. and Englaro, A. and Benini E., 2010. The darrieus wind turbine: Proposal for a new performance prediction model based on cfd. *Energy*, 36(8):4919-4934, 2011, ISSN 0360-5442.
- Rezaeiha, A. and Montazeri, H. and Blocken, B., 2019. On the accuracy of turbulence models for cfd simulations of vertical axis wind turbines. *Energy*, 180:838–857, 2019, ISSN 0360-5442.
- Holzmann, T., 2022 Vertical axis wind turbine. <https://holzmann-cfd.com/community/training-cases/vertical-axial-wind-turbine>, visited on September 4, 2022.